

A Novel Stem/Progenitor Cell Population from Murine Tracheal Submucosal Gland Ducts with Multipotent Regenerative Potential

Ahmed E. Hegab¹, Vi Luan Ha¹, Jennifer L. Gilbert¹, Kelvin Xi Zhang², Stephen P. Malkoski³, Andy T. Chon¹, Daphne O. Darmawan¹, Bharti Bisht¹, Aik T. Ooi¹, Matteo Pellegrini⁴, Derek W. Nickerson¹ and Brigitte N. Gomperts^{1,5,6,7}.

¹ Mattel Children's Hospital at UCLA, David Geffen School of Medicine at UCLA, Department of Pediatrics, Division of Hematology Oncology, Los Angeles, CA, 90095; USA.; ² Department of Biological Chemistry, Howard Hughes Medical Institute, David Geffen School of Medicine, University of California Los Angeles, Los Angeles, CA 90095; USA.; ³ Division of Pulmonary Sciences and Critical Care Medicine, University of Colorado Denver Health Sciences Center, Aurora, CO, USA.; ⁴ Department of Molecular, Cellular, and Developmental Biology, University of California, Los Angeles, CA, 90095; USA.; ⁵ Lung Cancer Research Program of the Jonsson Comprehensive Cancer Center, Los Angeles, CA, 90095; USA.; ⁶ Department of Medicine, Division of Pulmonary and Critical Care Medicine, David Geffen School of Medicine at UCLA, CA, 90095; USA.; ⁷ Eli and Edythe Broad Center of Regenerative Medicine and Stem Cell Research, UCLA, CA, 90095; USA.

Key words. airway epithelial repair and regeneration • lung stem cells • submucosal glands • hypoxic-ischemic injury

ABSTRACT

The airway epithelium is in direct contact with the environment and therefore constantly at risk for injury. Basal cells have been found to repair the surface epithelium, but the contribution of other stem cell populations to airway epithelial repair have not been identified. We demonstrated that airway submucosal gland duct cells, in addition to basal cells, survived severe hypoxic-ischemic injury. We developed a method to isolate duct cells from the airway. *In vitro* and *in vivo* models were used to compare the self-renewal and differentiation potential of duct cells and

basal cells. We found that only duct cells were capable of regenerating submucosal gland tubules and ducts, as well as the surface epithelium overlying the submucosal glands. Submucosal gland duct cells are therefore a multipotent stem cell for airway epithelial repair. This is of importance to the field of lung regeneration as determining the repairing cell populations could lead to the identification of novel therapeutic targets and cell-based therapies for patients with airway diseases.

INTRODUCTION

The airway epithelial cells of the conducting airways perform an essential role in innate host defense both by providing a physical barrier and by producing mucus and serous secretions that

allow the body to clear infectious agents and environmental toxins[1]. These airway epithelial cells are constantly at risk for injury as they are in direct contact with the environment. The ability of the airway surface epithelium (SE) to undergo efficient repair and functional

Author contributions: A.E.H.: Conception and design, Collection and/or assembly of data, Data analysis and interpretation, Manuscript writing; V.L.H.: Collection and/or assembly of data; J.L.G.: Collection and/or assembly of data; K.X.Z.: Data analysis and interpretation; S.P.M.: Provision of study material; A.T.C.: Collection and/or assembly of data; D.O.D.: Collection and/or assembly of data; B.B.: Data analysis and interpretation; A.T.O.: Data analysis and interpretation; M.P.: Data analysis and interpretation; D.W.N.: Collection and/or assembly of data, Data analysis and interpretation; B.N.G.: Conception and design, Collection and/or assembly of data, Data analysis and interpretation, Manuscript writing, Final approval of manuscript

Corresponding author: Brigitte N. Gomperts. 10833 Le Conte Ave., A2-410 MDCC, Los Angeles, CA, 90095. Telephone: 310-825-6708. Fax: 310-206-8089. e-mail: bgomperts@mednet.ucla.edu; Funding Sources: CIRM RN2-00904-1, K08 HL074229, American Thoracic Society/COPD Foundation ATS-06-065, The Concern Foundation, The UCLA Jonsson Comprehensive Cancer Center Thoracic Oncology Program/Lung Cancer SPORE, the University of California Cancer Research Coordinating Committee and the Gwynne Hazen Cherry Memorial Laboratories (BG).; Received April 27, 2011; accepted for publication June 02, 2011. ©AlphaMed Press 1066-5099/2011/\$30.00/0 doi: 10.1634/stem.680

regeneration is an important part of protection of the host.

The identity of all the resident stem or progenitor cells responsible for airway postnatal growth, homeostasis, and repair after injury remains under investigation [2-4]. Recently, lineage tracing and isolation of cell populations was used to provide compelling evidence that the majority of BCs in the trachea and Clara cells in the bronchi and bronchioles can self-renew and generate differentiated progeny of the SE [5,6].

The airway SE consists of many cell types, which have defined locations and cell markers (Fig 1). Basal cells (BCs) are classically rounded cells with low pyramidal nuclei and express cytokeratin (K)5 and p63. Secretory cells (Clara and serous cells) are identified by their columnar shape and expression of SCGB1A1 and the polymeric immunoglobulin receptor (pIgR), lysozyme and/or lactoferrin. Ciliated cells are identified by their characteristic columnar shape and cilia that stain positively for acetylated tubulins. There are also a lesser number of neuroendocrine cells and a few goblet cells in the airway epithelium. The vast majority of mucus and serous secretions are produced by the submucosal glands (SMGs) that are present in the submucosal region of the airway between the SE and the cartilage rings (Fig. 1A). SMGs consist of interconnected serous and mucus tubules, which are lined by polyhedral serous and mucus cells with rounded basal nuclei. Mucus can be detected in mucus cells with Alcian Blue/Periodic acid-Schiff staining (AB/PAS) and with DMBT1, while serous cells express lysozyme, lactoferrin and pIgR. SMG tubules are surrounded by flat, thin myoepithelial cells (MECs), which express K5, K14 and α -smooth muscle actin (α SMA). Serous and mucus tubules converge into collecting ducts that turn into ciliated duct before opening into the SE [7]. SMG duct cells characteristically express K5 and K14.

In human lungs, SMGs exist along the airways from the larynx down to the distal part of the

main bronchi. However, in mouse lungs, they are restricted to the upper trachea with the biggest bunch of glands being lodged between the cricoid cartilage and the first tracheal cartilaginous ring (C1 [8]).

SMGs and SMG ducts lie below the SE in the submucosal region of the airway, which is a relatively protected anatomical location in comparison to the SE. Label-retaining cells have been found to localize to the SMG and its ducts [9]. The ducts of other glandular tissues, such as breast and salivary glands, have been found to harbor adult stem/progenitor cell populations, suggesting the possibility of an analogous epithelial stem/progenitor cell in the SMG duct [10,11]. However, the potential contribution of SMG duct cells to airway epithelial repair has not been fully explored. The regenerative capacity of SMG duct cells is not known, as no techniques have existed up until now to selectively isolate the SMG duct cells to evaluate their stem cell properties.

Here we demonstrate the role of the SMG duct cell in regeneration of both the SMG tubules and the SE after severe hypoxic-ischemic injury. Using a novel method to isolate SMG duct cells from the airway, we utilize *in vitro* and *in vivo* stem cell model systems and lineage tracing to show that the SMG duct cells have the ability to self renew and differentiate into SMGs and SMG duct cells as well as to form the SE adjacent to the submucosal duct area.

MATERIALS AND METHODS

Mice

Wild-type C57BL/6, β -actin GFP (C57BL/6-Tg[ACTbEGFP]10sb), β -actin RFP (C57BL/6-Tg[ACTbERFP]1Nagy/J), ROSA26-floxSTOP-YFP (B6.129X1-Gt(ROSA)26Sor^{tm1(EYFP)Cos}/J) mouse strains were purchased from The Jackson Laboratory. Transgenic C57/BL6 K14-CrePR1 mice were made and kindly provided by Xiao Jing Wang. Mice were housed and bred under the regulation of the Division of Laboratory

Animal Medicine at the University of California, Los Angeles.

Mouse tracheal transplant model

We used a well-established, reproducible murine model of tracheal epithelial regeneration using syngeneic subcutaneous tracheal transplantation from C57BL/6 into C57BL/6 mice [12,13]. Tracheal grafts were collected from euthanized mice at post-transplant days 1 and 3, then formalin fixed and paraffin embedded.

***In vivo* SMG regeneration model**

5,000 sorted duct cells were directly injected into the fat pad around the scapular region of the mouse back. At collection of the grafts, the whole fat pad was excised and sectioned.

Immunostaining

Longitudinally embedded tracheas were cut from paraffin blocks ensuring the inclusion of any existing SMGs from below the larynx to at least C10. Spheres and ALI cultures were fixed in formalin, covered in Histogel® (Fisher Scientific), and then paraffin embedded and sectioned. Immunostaining was performed as described [14]. The primary antibodies used were chicken K15, rabbit K5 and K14 (Covance), Mouse p63, goat K5, SCGB1A1 and DMBT1 (Santa Cruz), rat ITGA6, rabbit NGFR, mouse and rabbit K14 (Abcam), goat TROP-2 and pIgR (R&D), chicken K8 (Novus Biologicals), rat EpCAM-647 (Biolegends), rabbit Lactoferrin (Upstate), Goat GFP (Rockland), rabbit lysozyme (kindly provided by Dr. Tom Ganz), mouse α SMA and acetylated β tubulin (Sigma) and Rat ITGA6-APC (e-bioscience). The appropriate Alexa-Fluor coupled secondaries were used in double and triple staining sections. Sections were counterstained with DAPI (Vector) and analyzed by fluorescent microscopy with a Zeiss AxioImager microscope (Carl Zeiss, Germany).

Separate isolation of mouse tracheal SE and SMG

Mouse whole tracheas were dissected then cut below tracheal ring C4 into upper and lower

parts. The lower part was processed for isolation of BCs as previously described [5] with modifications. Briefly, the lower two thirds of the tracheas were incubated for 30 minutes in 16 U/mL Dispase (BD Biosciences) at room temperature, then for 20 minutes in 0.5 mg/ml DNase (Sigma). The epithelium was peeled off with forceps under a dissecting microscope, and then incubated in 0.1% trypsin for 20 minutes at 37 °C to digest the peeled cell sheets into a single cell suspension. The upper parts were incubated in 0.15% Pronase (Roche) for 4 hours at 4 °C. The remaining tracheal pieces were washed twice to ensure complete removal of all peeled SE. The remaining tracheal pieces were minced with a fine scissors for 5 minutes to open up the SMG compartments and incubated with pronase for one hour, then washed and incubated in 0.1% trypsin for 20 minutes at 37 °C and passed through a 40 μ m cell strainer to obtain a single cell suspension.

FACS

Cells from SE were stained for TROP-2 and ITGA6 conjugated to PE or APC (eBioscience and Biolegend) and cells from SMG were stained for TROP-2 by incubation with the antibody for 15 minutes at room temperature followed by washing and incubation in donkey anti-goat Alexa Fluor 488 or PE. Sorting was performed on a FACS Aria and the data analyzed with FACS Diva software (BD Biosciences).

***In vitro* sphere cultures**

FACS-sorted cells were resuspended in MTEC/Plus media [15], and mixed 1:1 with growth factor-reduced Matrigel (BD Biosciences) [5]. The number of spheres per insert was counted on day 7. After 21 days in culture, spheres were embedded in Histogel and then in paraffin.

RNA extraction and amplification and microarray hybridization

Total RNA was extracted from sorted cell populations using RNeasy kits (Qiagen). per the manufacturer's protocol. Amplification of RNA

and subsequent microarray hybridization was performed following standard Affymetrix protocols.

Gene expression analysis

Raw gene expression data (.cel files) were generated by standard Affymetrix protocols and deposited in the Gene Expression Omnibus of the National Center for Biotechnology Information (accession number GSE28651). The import and normalization of the raw data were completed by Bioconductor in the R software environment. Two types of statistical tests (t-test and rank product) were performed for each probe set in order to detect differentially expressed genes between the BCs and the duct cells. For both methods, only genes with an adjusted P-value < 0.01 and fold change ≥ 2 based on the false discovery rate were considered as differentially expressed genes and were annotated. Gene expression patterns of highly differentially expressed genes (the top 100 genes derived from the rank product methods) were compared by the heatmap function in R. We used the Database for Annotation, Visualization and Integrated Discovery (DAVID) [16] and the Ingenuity Pathways Analysis (IPA) database (Ingenuity® Systems, <http://www.ingenuity.com>) to analyze biological functions and pathways of these highly differentially expressed genes.

Lineage tracing

For lineage tracing experiments, 5–8 week-old mice hemizygous for *KRT14-CrePR1* and homozygous for *Rosa26-YFP*, received intratracheal injections with 500 μ g RU486 in 25 μ l of 20% acetone/80% sunflower oil using 0.3 ml insulin syringes (BD). Control mice received injections of only acetone/oil. Six days later, the mice were euthanized and their tracheas were collected, immersed in RU486 for 10 minutes and then transplanted heterotopically, as described above.

Statistics

All experiments were performed with at least three different primary cultures or mice in independent experiments. Significance was evaluated by Student's t-test. Data are presented as mean \pm SD.

RESULTS

SMG duct cells and a few BCs survive severe hypoxic ischemic injury and are therefore the likely source of repair of the SE, SMGs and SMG ducts

The syngeneic, heterotopic murine tracheal transplant model results in interruption of the blood supply and causes a severe hypoxic-ischemic injury. In this model, complete *in vivo* regeneration of the trachea SE, SMGs and SMG ducts occurs within 2-3 weeks [12,13]. We hypothesized that the epithelial cells that survived this injury would be the stem/progenitor cells responsible for airway epithelial repair and regeneration. Extensive injury was seen on day 1 that reached its maximum on day 3 post-transplantation, as most of the SE and SMG cells sloughed off into the tracheal and ductal lumens and large areas of the basement membrane were denuded (Fig 1Bii). Widespread expression of Annexin V, a marker of cell death, was seen in the SE and SMGs (Fig 1Biii). In the SMGs, MECs, as well as mucus and serous tubules all became atrophic forming anuclear halos. The only cells that survived this injury were the K5+K14+ SMG duct cells and occasional K5+K14- BCs (Fig 1Bii, iii).

The significant repair from only a few viable cells that was seen in this injury/repair model implies that these surviving cells contain the stem/progenitor cell populations for regenerating the pseudostratified SE, SMGs and SMG ducts. As the only surviving epithelial cell populations in this model were some BCs and the SMG duct cells, we sought to characterize and compare the self-renewal and differentiation potential of each of these cell populations.

Isolation of SMG duct cells separate from BCs

In order to find specific markers to isolate the SMG duct cell population separately from the BC population, we first performed immunofluorescent staining for known markers of epithelial cell populations in the trachea. We found that the previously described [5] markers of airway BC, nerve growth factor receptor (NGFR) and integrin- α -6 (ITGA6), were expressed in both BCs as well as SMG duct cells, but were not expressed in MECs or tubule cells of the SMGs (Fig 2Ai and ii). EpCAM was expressed on all epithelial cells of the airway (Fig 2Aiii). TROP-2, a previously described marker of prostate basal cells, [17], was expressed on all cells of the SE as well as the duct cells, but not in MECs or tubule cells of the SMGs (Fig 2Aiii and iv).

Based on the pattern of TROP-2 expression, we decided to use enzymatic digestion of the trachea to completely remove the SE, including all BCs, followed by fluorescence-activated cell sorting (FACS) sorting of the remaining trachea for TROP-2+ duct cells, thus excluding SMG tubular, MEC and non-epithelial stromal cells. Previous studies have used overnight protease XIV (pronase) [2,9,18] or 30 minutes of dispase [5] enzyme digestion to strip the SE from the rest of the tracheal tissues. We performed a time course of digestion of the tracheal epithelium with pronase and found that 4 hours of digestion with pronase removed the SE without removing duct cells. However, longer time points of 8, 12 and 16 hours all removed duct cells in addition to BCs (Supplemental data Fig S1).

We therefore exposed the upper third of mouse tracheas to 4 hours of pronase digestion to selectively remove the SE with the BCs, and then performed FACS of the single cell suspension obtained from the remaining tracheal tissue, using a primary antibody for the surface marker, TROP-2 (Fig 2Bi). We found that 20% of total tracheal cells, after removing the SE, expressed TROP-2 and represented duct cells (Fig 2Bi).

We found that SE collected from the trachea using pronase could not be used for BC sorting as it removed the surface epitopes of ITGA6 and NGFR preventing their use in FACS. We therefore performed tracheal digestion with dispase, but found that just 30 minutes was sufficient to strip not only the SE, but also considerable parts of the SMG ducts and tubules (Supplemental data Fig S2). Therefore, as SMGs in mice are only present in the upper third of the mouse trachea [8], we used dispase digestion of only the lower two-thirds of mouse tracheas to remove the SE to obtain a single cell suspension for FACS, specifically for BCs, using TROP-2 and ITGA6 (Fig 2Bii). We found 35% of SE cells were TROP-2+ITGA6+ BCs.

TROP-2+ duct cells can self renew and differentiate into the cell types of the SMG duct, SMG tubules and SE under in vitro culture conditions.

To assess the ability of TROP-2+ duct cells to self-renew and differentiate *in vitro*, we used the 3-dimensional sphere-forming assay that has been described for stem cells from the brain [19], prostate [17], distal lung [20,21] and airway BCs [5]. TROP-2+ duct cells that were plated in matrigel produced an overall efficiency of colony formation of $0.67 \pm 0.25\%$ when duct cells were plated anywhere in the range of 10,000 to 60,000 cells per well. Two different morphologic types of TROP-2+ duct spheres were seen after 21 days in culture. The first consisted of a dense ball of cells with little or no central lumen. The second had a large central lumen with 2-3 cell layers lining the sphere which were reminiscent of BC-derived tracheospheres [5] (Fig 3A i, ii). The size of the spheres varied from 50-300 microns with the spheres with larger lumen size being typically wider in diameter. Of the two types of spheres, 95% were dense spheres, and 5% were luminal spheres. To assess clonality, TROP-2+ duct cells from ubiquitously expressing GFP mice (β -actin-GFP, Jackson labs) and wild-type mice were mixed 1:1 and colonies were examined for expression of GFP. The cells making up an individual colony were either all GFP+ or all wild-type confirming that

these colonies are clonally derived from a single TROP-2+ duct cell, rather than by aggregations of sorted cells, which would give rise to mixed color colonies (Fig 3Aiii). Control TROP-2 negative cells from the tracheas that contained the epithelial tubular cells, MECs and stromal cells did not generate spheres in culture.

TROP-2+ITGA6+ BCs sorted from the lower two-thirds of the tracheal SE, to ensure no contamination with duct cells, produced a clonal efficiency of $2.1 \pm 0.6\%$ when plated in the range of 10,000 to 60,000 cells per well. These cells differentiated into only the luminal type of spheres (Fig 3Av, vi) and these spheres were also clonal (Fig 3A vii). TROP-2+ITGA6- FACS sorted cells did not form spheres.

To determine the differentiation ability of the TROP-2+ duct cells we examined expression in the spheres for proteins characteristic of differentiated cell types of the SE and the SMGs and ducts. Dense spheres from SMG duct cells, expressed K5 and K14 (Fig 3Bi). The spheres also expressed K15, but did not express tubulin, SCGB1A1 or α SMA (Fig 3Bii). K8 was expressed in the cells in the center of the dense spheres in $48.25 \pm 26\%$ of spheres (Fig 3Biii). Dense spheres demonstrated two patterns of p63 expression; one pattern showed nuclear p63 expression was only present in the basal layer of the sphere and in the other pattern it was expressed in all the cells of the dense sphere (Fig 3Biv, v). A subset of the dense spheres ($13.3 \pm 5.1\%$) also expressed the serous cell marker, pIgR (Fig 3Bvi) and there were spheres that stained positively for the mucus stain, AB/PAS ($8.33 \pm 8.28\%$) (Fig 3Aiv). TROP-2 was expressed on all cells of the dense spheres (Fig 3Bvii). The SMG duct cell spheres have been passaged up to four times and have the same efficiency of sphere formation, the same dense sphere morphology and equivalent differentiation ability.

FACS sorted BCs produced spheres with a basal layer of K5 and K14 expressing cells (Fig 3Bviii). K15, luminal K8 and nuclear p63

expression was also seen (Fig 3B ix, x and xi). BC spheres expressed tubulin in $60 \pm 11.52\%$ of spheres (Fig 3B xii) and a subset of the BC spheres expressed the serous cell marker, pIgR ($56.2 \pm 25.2\%$) (Fig 3B xii). The BC spheres did not express SCGB1A1 or α SMA. TROP-2 was present in all cells of the basal spheres (Fig 3Bxiii). A subset of basal spheres produced mucus as detected by AB/PAS ($28.5 \pm 7.39\%$) (Fig 3Aviii).

The duct luminal spheres and the basal luminal spheres therefore had very similar differentiation capabilities, but duct luminal spheres did not differentiate into ciliated cells, unlike basal luminal spheres. We further compared the differentiation potential of duct and basal cells in air-liquid interface cultures and found that they had very similar potential to form mucus and serous cells and that in this system duct and basal cells had the same potential to differentiate into ciliated cells (Supplemental data Figure S3).

TROP-2+ SMG tracheal duct cells and TROP-2+ITGA6+ BCs have gene expression profiles that differ in key genes related to epithelial differentiation

We extracted RNA from FACS sorted cells from TROP-2+ SMG duct tracheal cell populations as well as SE TROP-2+ITGA6+ tracheal BCs. RNA from the 2 populations was analyzed on the Affymetrix microarray platform. Of the 45,101 genes profiled in the gene expression data, 788 probes representing 776 genes with false discovery rate (FDR)-adjusted p-value of < 0.01 and fold change ≥ 2 were identified as being differentially expressed between the BCs and the duct cells by the t-test. Among these 776 genes, 528 (68%) were upregulated and 248 (32%) were downregulated in the duct cells. We clustered and displayed the 100 most differentially expressed genes to demonstrate that their transcription profiling patterns are substantially different between the BCs and the duct cells, while their patterns are quite similar within replicates (Fig. 4A). In addition, we adopted a non-parametric statistical method (the Rank Product) to the same data set and identified

74 differentially expressed genes (adjusted P-value < 0.01 and fold change ≥ 2). We found that these 74 differentially expressed genes belong to a subset of the 788 significant genes. Pathway analysis revealed enrichment in genes in duct cells compared to BCs that were related to epithelial development and more specifically to the development of stratified squamous epithelium, such as the skin. Such genes include the stratified epithelium-related gene cluster, termed the stratified epithelium secreted peptides complex, which harbors at least three genes encoding for the secreted peptides, dermokinase (*Dmkn*), keratinocyte differentiation-associated protein (*Krt14*), and suprabasin (*Sbsn*). One pathway was identified with genes that were upregulated in the SMG duct compared to BCs that are associated with dermatologic conditions and diseases and genetic disorders (Fig. 4B). Some genes of interest from this pathway included desmoglein (*Dsg1*), a core component of desmosomes, and Insulin-Like Growth Factor Binding Protein-4 (*Igfbp4*).

We also compared the transcription profiles of the BCs in this study to those of a population of FACS isolated lectin⁺;KRT5-GFP⁺ BCs in a previous study [5] and found that they were similar (Pearson correlation coefficient of 0.851).

We performed quantitative real-time PCR of some candidate genes found to be differentially expressed in basal and duct cells and confirmed that *K5*, *K14*, *Igfbp4*, and *Asprv1* have significantly higher expression in duct than in basal cells ($p < 0.005$) (Fig. 4C). Immunostaining for IGFBP4 and ASPRV1 followed the same pattern of increased protein expression in duct compared to basal cells (Fig. 4D).

TROP-2+ duct cells can self renew and differentiate into SMG duct-like and SMG tubule-like structures in an *in vivo* transplantation system

To create an *in vivo* model of self-renewal and differentiation of airway epithelial stem/progenitor cells, we sought to recapitulate

other *in vivo* adult stem cell model systems like the mammary fat pad and renal capsule models [22-24]. We injected sorted TROP-2+ duct cells from RFP transgenic mice, into the fat pad around a recipient wild-type mouse scapula. We found that in 50% of the injected mice, SMG duct cells could organize themselves into SMG tubule-like structures (Figure 5i, iii) that were RFP⁺ (i.e. of donor origin, Figure 5i). These structures expressed K5 and K14 (Figure 5ii,v) and were functional tubules as they expressed the serous cell marker lysozyme (Figure 5vi) and mucus with positive staining for AB/PAS (Figure 5iv). In addition, these SMG tubule-like structures contained α -SMA and K14 expressing cells in a pattern consistent with the development of myoepithelial cells (Figure 5v, vi). In 20% of these grafts SMG duct-like structures were seen in addition to the typical SMG tubule-like structures (Figure 5ii). This indicates that SMG duct cells can reconstitute functional SMG-like structures *in vivo* and that placing single duct cells in the dorsal fat pad niche represents a novel model to study the regeneration of SMG tubules and ducts.

Lineage tracing shows K14-expressing SMG duct cells contribute to the repair of the SE as well as the SMG and SMG duct after hypoxic-ischemic injury

In naïve mouse tracheas, cells that express K14 are only located in the SMG ducts and MECs, while less than 10% of SE BCs express K14 (Figures 6i and [14]). In order to examine whether SMG duct cells participate in regenerating the SE, we performed lineage tracing of K14⁺ cells in transgenic mouse tracheas. We utilized a transgenic mouse model that selectively induces YFP expression in K14⁺ cells. K14CrePR1 mice [25] were bred with C57/BL6 ROSA26-floxSTOP-YFP mice (Jackson labs). Because steady state tracheal epithelial turnover is known to be very slow, we performed the lineage tracing using the same hypoxic-ischemic injury model we described above.

RU486 or vehicle control was administered intratracheally as previously described [25] on day 0. On day 6, tracheas were harvested from these transgenic mice and immersed in RU486 or vehicle control, before being transplanted heterotopically into syngeneic wild-type recipient mice. The tracheal transplants were harvested 7 days later and immunostaining was performed for YFP and K14 expression. The timing of the dosing of RU486 was such that only the surviving K14⁺ duct cells and the few K14⁺ BCs of the steady state SE would have been subject to induction of Cre-recombinase and therefore expression of YFP. Cells that turned on K14-expression as part of the repair process would therefore not have been exposed to RU486 and induction of Cre-recombinase. Vehicle control treated tracheas did not show any evidence of YFP expression. At 7 days post-transplantation, YFP expression was found in the SMGs, SMG ducts and the SE adjacent to and overlying the SMG ducts (Figure 6ii, iii). In the lower two-thirds of the trachea, which does not have SMGs, a few randomly scattered foci of YFP+K14⁺ cells were seen in the SE (Figure 6iv) likely reflecting induction of YFP expression in a few K14⁺ BCs. Quantification of YFP⁺ SE derived from K14⁺ SMG duct cells demonstrated that SMG duct cells gave rise to 25-30% of the airway epithelium of the upper third of the trachea. By comparison, the YFP⁺ SE only represented <5% of the tracheal surface area in the lower two thirds of the trachea. This indicates that SMG duct cells do participate in repairing the SE in the presence of BCs.

DISCUSSION

Our data shows that SMG duct cells are a population of multipotent stem/progenitor cells that survive a severe hypoxic-ischemic injury in the tracheal epithelium and play a role in repair of the SMGs, SMG ducts and SE analogous to the identification of stem cell populations in the ducts of other tissues [10,11]. We developed a novel method to isolate SMG duct cells by FACS and used *in vitro* and *in vivo* models of stem/progenitor cell self-renewal and

differentiation to compare the regenerative potential of known stem/progenitor cells in the airway SE, namely the BCs, to the SMG duct cells. We found that unlike BCs, SMG duct cells were capable of repairing the SMG serous and mucus tubules and MECs and that they were also able to regenerate SE. We speculate that previous reports of surface airway epithelial cell and BC self-renewal and differentiation ability may have been affected by enzymatic digestion methods that also allowed duct cells to be included with BC preparations [2,5,18,26]. This likely explains why air-liquid interface cultures from the proximal half of the mouse trachea are more efficient at making airway epithelium than the distal half, which has no submucosal glands and ducts, but both halves are capable of generating differentiated airway epithelium in culture [27]. We believe that our data demonstrate that basal cells and duct cells both contain stem/progenitor cells, but that within duct cells there is a more multipotent stem/progenitor cell.

We found important similarities and differences between the SMG duct stem/progenitor cell population and the BC stem/progenitor population. The SMG duct cells are distinct from the BCs in that 1) they give rise mostly to dense clonal spheres in culture, 2) they are capable of generating SMG-like structures in an *in vivo* model of regeneration, 3) lineage tracing shows that this population forms SMGs, SMG ducts and SE adjacent to the SMG ducts and 4) microarray analysis demonstrates key differences in the nature of the epithelium of the duct cells as compared to BCs. However, there are also similarities between the SMG duct and BC stem/progenitor populations, 1) they both express the surface markers ITGA6 and NGFR, and 2) in the sphere-forming and air-liquid interface assays, they have similar differentiation capacity.

SMG duct cells express K14 and we showed previously that under steady state conditions, only 10% of mouse BCs and just 1% of human BCs of the SE express K14 [14]. However,

pre-malignant lesions of the SE all express K14 and the presence of K14 in primary non-small cell lung cancer (NSCLC) tissue was associated with a poor prognosis [14]. The presence of K14 in the airway epithelium therefore appears to correlate with response to injury and the presence of stratified rather than pseudostratified epithelium. The microarray gene expression profile comparison of SMG duct and BCs demonstrates that the duct cells are programmed towards stratified squamous epithelium and express genes that are associated with stratified squamous epithelial cancers, such as squamous skin cancer. This leads us to speculate that SMG duct cells may be a stem cell of origin for NSCLC. We further hypothesize that because duct cells can give rise to glandular structures (the submucosal glands), as well as surface epithelium, that it is possible that they could give rise to NSCLCs with both squamous and adenocarcinoma histologies.

In mice the SMGs and SMG ducts are only present in the upper third of the trachea [8] and the SMG duct cells, therefore, likely do not play the major role in repair of the airway epithelium. However, in other mammals such as pigs and humans, SMGs and SMG ducts are found throughout the cartilaginous airways and it is therefore possible that SMG ducts play a larger role in repair of the airway SE, in addition to repair of the SMGs and SMG ducts after injury in humans. There are a number of clinical scenarios where injury results in sloughing of the SE, for example in respiratory syncytial virus infection or acute smoke inhalation. We envision that the SMG duct cells will play an important role in repair of the airway epithelium in these situations.

A normal human bronchial epithelial cell line (Clonetics cell systems, Lonza, Walkersville, MD) has been shown to generate spheres and possess self-renewal and differentiation potential in matrigel cultures [28]. These spheres were able to differentiate to mucus and serous cell types and produced luminal spheres in culture. However, it is not clear whether SMG duct cells

might be included in the culture system, as the nature of the human samples used to generate these cell lines is proprietary information. Based on our studies, it seems likely that SMG duct cells as well as BCs are included in these cell preparations

A similar strategy of lineage tracing K14-expressing cells in the airway has been recently published [29]. Although the investigators did not focus on SMGs or SMG ducts, they did comment that they detected cells derived from K14+ cells in the SMG tubules and ducts but not in the SE adjacent to the glands. Two aspects of this previous study hampered the investigators' ability to assess the role of SMG ducts in repair and regeneration of the airway epithelium. Firstly, the authors found that endogenous B-galactosidase activity was present in peritracheal glands and they could therefore not perform lineage tracing in these areas. Secondly, the naphthalene model of airway epithelial injury used in the study is not as severe an injury as the hypoxic-ischemic tracheal transplant model and may not therefore require the recruitment of SMG duct cells for repair of the SE.

We found that SMG duct cells have about a four-fold lower colony generating capacity than BCs. There are a number of possible explanations for this. One major reason is that SMG duct cells are comprised of at least three distinctive cell populations, namely, BCs of the duct (ITGA6+/NGFR+/Tubulin-), ciliated cells of the duct (ITGA6-/NGFR-/Tubulin+), and non-ciliated, non-BCs of the duct (ITGA6-/NGFR-/Tubulin-). It is possible that only one of these cell populations is the genuine stem/progenitor cell and thus with our current method of sorting all TROP-2+ duct cells, we are only obtaining a population that is enriched for the true duct stem/progenitor cell. Another possible explanation is that SMG duct cells are in a more protected location and not exposed to constant environmental injury, as the BCs are. They, therefore, only need to be recruited for repair in the setting of a severe injury and so may cycle more slowly.

Recently a stem cell was identified in the lung that appears to have the potential to differentiate into a number of different cell types of the proximal and distal airway epithelium as well as into the lung vasculature [30]. If this work can be replicated, then it suggests that there is a lineage hierarchy in the lungs and that duct cells are considerably further down the lineage than these lung stem cells

CONCLUSION/SUMMARY

We have identified a novel multipotent stem/progenitor cell in the SMG duct in the airway epithelium. This is of major importance to the field of lung regeneration. SMG hypertrophy is associated with airway inflammation and excessive mucus secretions, which are frequently seen in patients with chronic asthma, chronic obstructive pulmonary disease (COPD) and cystic fibrosis [1]. Our

ability to identify the SMG duct cells and their regenerative ability has implications for the possible identification of novel therapeutic targets for airway diseases and potential cell-based therapies in the future.

ACKNOWLEDGMENTS

We would like to acknowledge the UCLA Clinical Microarray Core and the Broad Stem Cell Research Center FACS Core. We would like to thank Jessica Scholes and Felicia Codrea for their help with cell sorting. We would like to thank Dr. Gay Crooks for her help with the manuscript. We would also like to acknowledge Xiao Jing Wang who provided us with the K14CrePR1 mice.

Disclosure of Potential Conflicts of Interest

There are no conflicts of interest.

REFERENCES

1. Bartlett JA, Fischer AJ, McCray PB, Jr. Innate immune functions of the airway epithelium. *Contrib Microbiol* 2008;15:147-63.
2. Schoch KG, Lori A, Burns KA, Eldred T, Olsen JC, Randell SH. A subset of mouse tracheal epithelial basal cells generates large colonies in vitro. *Am J Physiol Lung Cell Mol Physiol* 2004;286:L631-42.
3. Hong KU, Reynolds SD, Watkins S, Fuchs E, Stripp BR. In vivo differentiation potential of tracheal basal cells: evidence for multipotent and unipotent subpopulations. *Am J Physiol Lung Cell Mol Physiol* 2004;286:L643-9.
4. Hong KU, Reynolds SD, Watkins S, Fuchs E, Stripp BR. Basal cells are a multipotent progenitor capable of renewing the bronchial epithelium. *Am J Pathol* 2004;164:577-88.
5. Rock JR, Onaitis MW, Rawlins EL, et al. Basal cells as stem cells of the mouse trachea and human airway epithelium. *Proc Natl Acad Sci U S A* 2009;106:12771-5.
6. Rawlins EL, Okubo T, Xue Y, et al. The role of Scgb1a1+ Clara cells in the long-term maintenance and repair of lung airway, but not alveolar, epithelium. *Cell Stem Cell* 2009;4:525-34.
7. Meyrick B, Sturgess JM, Reid L. A reconstruction of the duct system and secretory tubules of the human bronchial submucosal gland. *Thorax* 1969;24:729-36.
8. Rawlins EL, Hogan BL. Intercellular growth factor signaling and the development of mouse tracheal submucosal glands. *Dev Dyn* 2005;233:1378-85.
9. Borthwick DW, Shahbazian M, Krantz QT, Dorin JR, Randell SH. Evidence for stem-cell niches in the tracheal epithelium. *Am J Respir Cell Mol Biol* 2001;24:662-70.
10. Visvader JE. Keeping abreast of the mammary epithelial hierarchy and breast tumorigenesis. *Genes Dev* 2009;23:2563-77.
11. Kimoto M, Yura Y, Kishino M, Toyosawa S, Ogawa Y. Label-retaining cells in the rat submandibular gland. *J Histochem Cytochem* 2008;56:15-24.
12. Gomperts BN, Belperio JA, Rao PN, et al. Circulating progenitor epithelial cells traffic via CXCR4/CXCL12 in response to airway injury. *J Immunol* 2006;176:1916-27.
13. Genden EM, Iskander A, Bromberg JS, Mayer L. The kinetics and pattern of tracheal allograft re-epithelialization. *Am J Respir Cell Mol Biol* 2003;28:673-81.
14. Ooi AT, Mah V, Nickerson DW, et al. Presence of a putative tumor-initiating progenitor cell population predicts poor prognosis in smokers with non-small cell lung cancer. *Cancer Res* 2010;70:6639-48.

15. You Y, Richer EJ, Huang T, Brody SL. Growth and differentiation of mouse tracheal epithelial cells: selection of a proliferative population. *Am J Physiol Lung Cell Mol Physiol* 2002;283:L1315-21.
16. Huang da W, Sherman BT, Lempicki RA. Systematic and integrative analysis of large gene lists using DAVID bioinformatics resources. *Nat Protoc* 2009;4:44-57.
17. Goldstein AS, Lawson DA, Cheng D, Sun W, Garraway IP, Witte ON. Trop2 identifies a subpopulation of murine and human prostate basal cells with stem cell characteristics. *Proc Natl Acad Sci U S A* 2008;105:20882-7.
18. Engelhardt JF, Yankaskas JR, Wilson JM. In vivo retroviral gene transfer into human bronchial epithelia of xenografts. *J Clin Invest* 1992;90:2598-607.
19. Reynolds BA, Weiss S. Generation of neurons and astrocytes from isolated cells of the adult mammalian central nervous system. *Science* 1992;255:1707-10.
20. McQualter JL, Yuen K, Williams B, Bertoncello I. Evidence of an epithelial stem/progenitor cell hierarchy in the adult mouse lung. *Proc Natl Acad Sci U S A* 2010;107:1414-9.
21. Inayama Y, Hook GE, Brody AR, et al. The differentiation potential of tracheal basal cells. *Lab Invest* 1988;58:706-17.
22. Xin L, Ide H, Kim Y, Dubey P, Witte ON. In vivo regeneration of murine prostate from dissociated cell populations of postnatal epithelia and urogenital sinus mesenchyme. *Proc Natl Acad Sci U S A* 2003;100 Suppl 1:11896-903.
23. Vu TH, Alemayehu Y, Werb Z. New insights into saccular development and vascular formation in lung allografts under the renal capsule. *Mech Dev* 2003;120:305-13.
24. Shackleton M, Vaillant F, Simpson KJ, et al. Generation of a functional mammary gland from a single stem cell. *Nature* 2006;439:84-8.
25. Malkoski SP, Cleaver TG, Lu SL, Lighthall JG, Wang XJ. Keratin promoter based gene manipulation in the murine conducting airway. *Int J Biol Sci* 2010;6:68-79.
26. Engelhardt JF, Schlossberg H, Yankaskas JR, Dudus L. Progenitor cells of the adult human airway involved in submucosal gland development. *Development* 1995;121:2031-46.
27. You Y, Richer EJ, Huang T, Brody SL. Growth and differentiation of mouse tracheal epithelial cells: selection of a proliferative population. *American journal of physiology Lung cellular and molecular physiology* 2002;283:L1315-21.
28. Wu X, Peters-Hall JR, Bose S, Pena MT, Rose MC. Human Bronchial Epithelial Cells Differentiate to 3D Glandular Acini on Basement Membrane Matrix. *Am J Respir Cell Mol Biol* 2010.
29. Ghosh M, Brechbuhl HM, Smith RW, et al. Context-Dependent Differentiation of Multipotential Keratin 14-Expressing Tracheal Basal Cells. *Am J Respir Cell Mol Biol* 2010.
30. Kajstura J, Rota M, Hall SR, et al. Evidence for human lung stem cells. *N Engl J Med* 2011;364:1795-806.

See www.StemCells.com for supporting information available online.

Figure 1. A. Schematic of the airway epithelial cell types of the cartilaginous airways.

Figure 1B. A few BCs and SMG duct cells are the only cells that survive the hypoxic-ischemic injury. Syngeneic heterotopic murine tracheal transplantation was performed, and transplanted tracheas were collected and examined on day 3 when there is maximal cell death. (n=4-6 tracheas per time point). A longitudinal section of a naïve trachea immunostained with K5, demonstrates the pseudostratified SE and the SMG ducts (yellow arrows) of the upper trachea (i). Only SMG duct (white arrows) and a few scattered BCs on the SE survived the hypoxic-ischemic injury. Wide areas of the BM were denuded and the few cells that remained attached to the BM were K5 positive. SMG ducts were lined with K5+ cells while SMG tubules and MECs were necrotic (ii, iii). Annexin V expression was seen in the sloughed cells in the lumen, SMG tubules and ducts (iii).

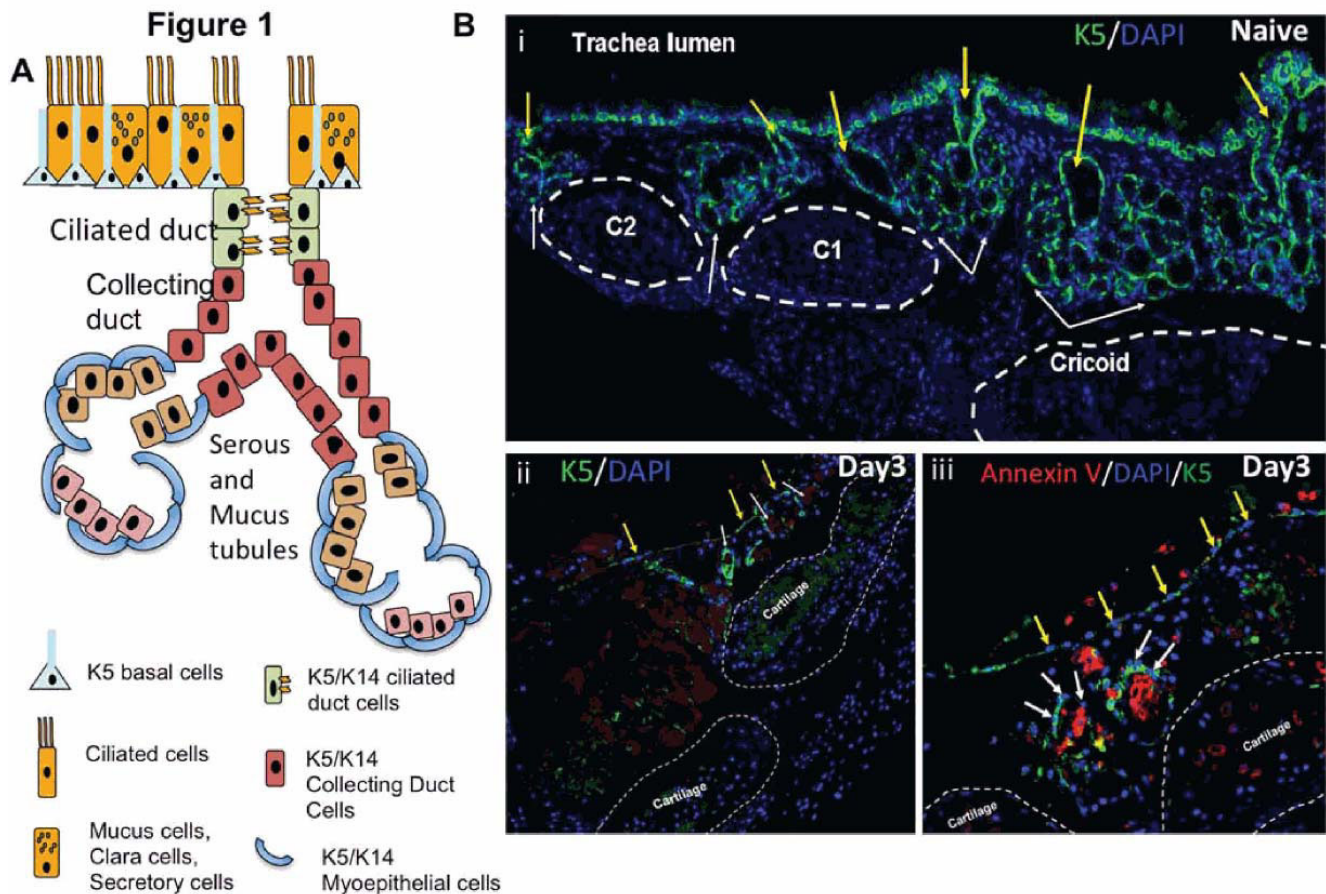


Figure 2. Characterization and isolation of SMG duct cells.

A. Immunofluorescent staining of SMG duct cells with primary antibodies for specific surface markers. ITGA6 and NGFR are expressed in BCs and are also expressed in the SMG duct (i, ii). EpCAM is present on all epithelial cells of the SE, SMG tubules and SMG duct, but TROP-2 is expressed in the cells of the SE and SMG duct, but not in the SMG tubules (iii, iv). K14 is expressed in SMG duct cells, and MECs of the tubules (iv).

B. FACS of SMG duct and BC populations. (i) The scatter plot shows the distribution of the tracheal cells remaining after stripping of the SE, i.e. SMG ducts, tubules and surrounding stroma. TROP-2+ duct cells (blue) and TROP-2- non-duct cells (green) were sorted. Duct cells represented 20% of the total cells.

(ii) The scatter plot shows the distribution of the stripped tracheal surface epithelial cells. TROP-2+ITGA6+ BCs (green) and TROP-2+ITGA6- non-BCs (red) were sorted. BCs represented about 35% of the total cells.

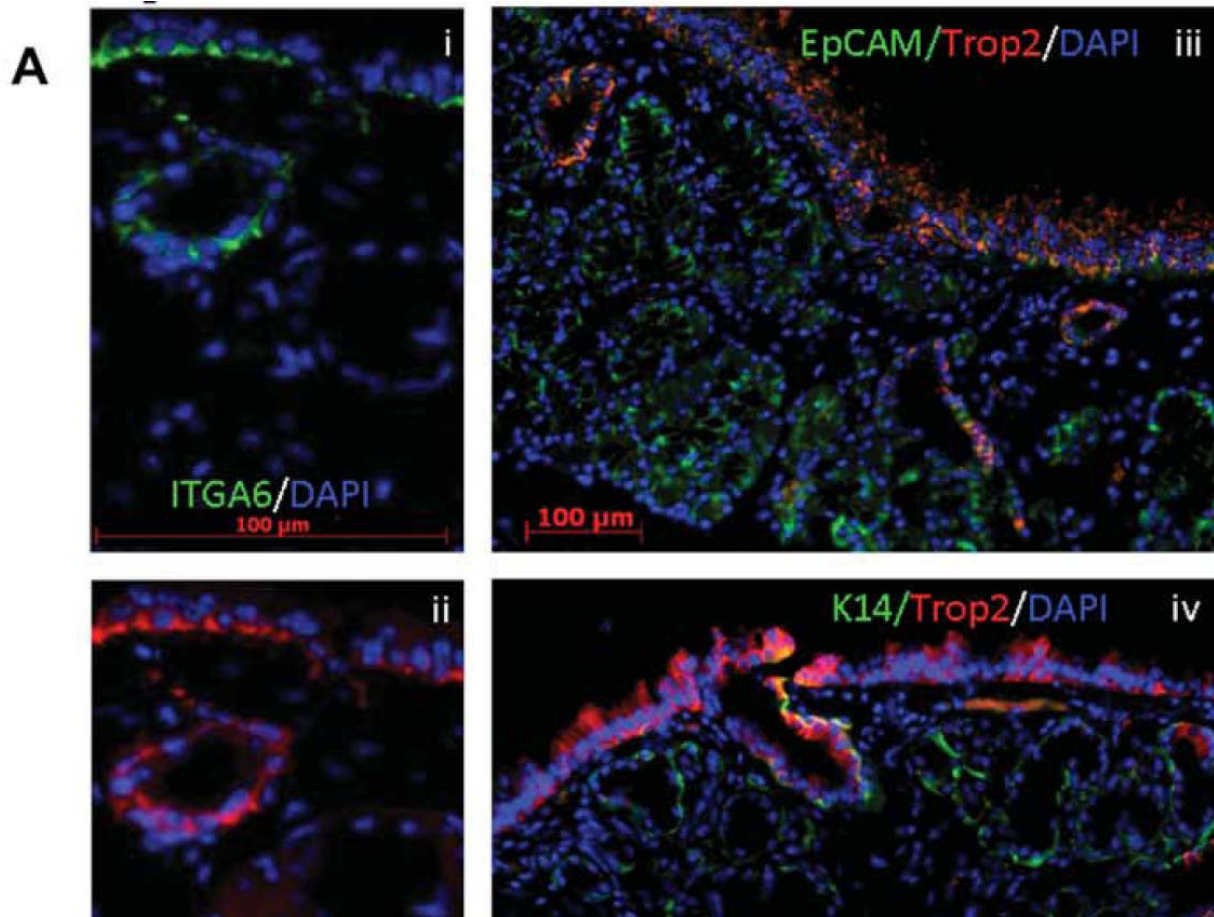


Figure 3. *In vitro* self-renewal and differentiation ability of SMG duct cells compared to BCs.

A. The sphere-forming assay: Sphere morphology, clonality and ability to synthesize mucin. Sorted TROP-2+ SMG duct cells were capable of generating spheres *in vitro*. Morphologically, two different kinds of spheres were generated; luminal type spheres (i-left) and dense spheres with little or no lumen (i-right). The dense spheres were generally smaller in diameter than the luminal spheres and ranged in size from 20-100µm. The luminal spheres ranged from 50-300µm. H&E of a cross section of the spheres demonstrated the lack of a central lumen in the dense spheres as compared to the luminal spheres (ii). Mixed 1:1 ratio of GFP:wild-type sorted duct cells demonstrated only green or wild-type spheres, indicating that spheres arose clonally from a single stem/progenitor cell (iii). Sorted duct cells produced mucus in the sphere cultures as seen by AB/PAS staining (iv).

Sorted TROP-2+ITGA6+ BCs from the SE also generated spheres *in vitro*. Morphologically, there were just luminal spheres, which varied in size from 50-300µm (v, vi). Mixed 1:1 ratio of GFP:wild-type sorted BCs demonstrated only green or wild-type spheres, indicating that spheres arose clonally from a single stem/progenitor cell (vii). Sorted BCs produced mucus in the sphere cultures as seen by AB/PAS staining (viii).

B. The sphere-forming assay: Differentiation ability.

Dense spheres from duct cells expressed K5 and K14 in all the cells of the sphere (i), with K5 being more strongly expressed on the outside (basal side) of the sphere, with K14 being strongly expressed on the inside (luminal side) of the sphere. K15 was expressed in all cells of the sphere (ii). 48.25±26% of the dense spheres expressed K8 in a luminal pattern (iii). p63 was found in two patterns, either on the basal surface or throughout the dense sphere (iv, v). 13.3±5.1% of spheres expressed the serous cell marker, pIgR (vi). TROP-2 was found on all cells of the sphere (vii).

The basal spheres expressed K5 and K14 in almost all the cells of the sphere (viii). p63 was found in cells located on the periphery (xi) and 100% of the spheres expressed K8 in a central pattern (x). K15 was expressed equally in all cells of the sphere (ix). 56.2±25.2% of spheres expressed the secretory marker, pIgR, and 60±11.52% expressed the ciliated marker, acetylated β-tubulin (xii). TROP-2 was found on all cells of the spheres (xiii).

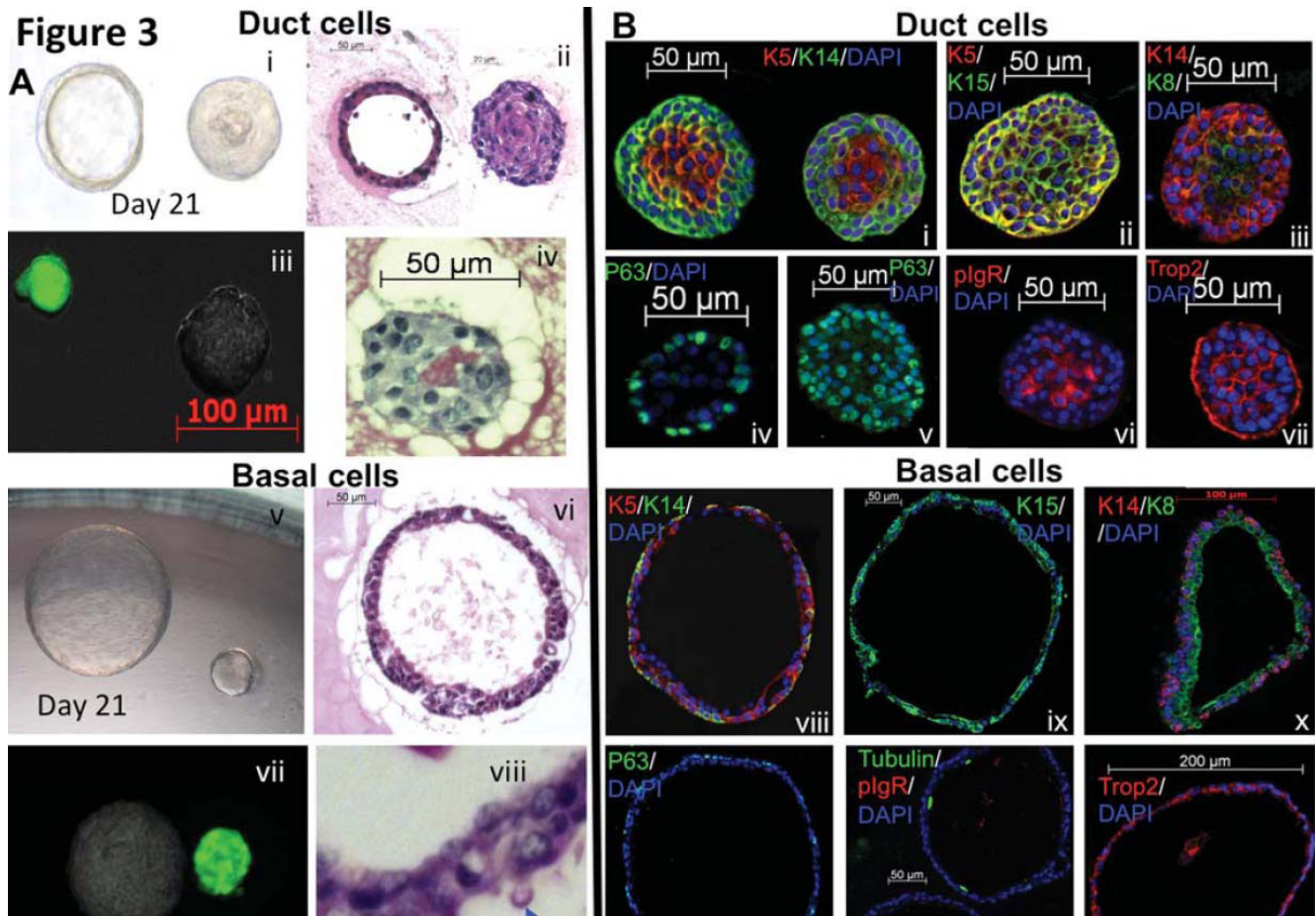


Figure 4. Gene expression profiling of SMG duct cells compared with BCs.

A. The heatmap shows the 100 most differentially expressed genes between sorted duct and BCs and demonstrates that their transcriptional profile is substantially different between the BCs and the duct cells, while their patterns are quite similar within replicates.

B. The Ingenuity Pathways Analysis (IPA) database was used to analyze biological functions and pathways of the 74 most highly differentially expressed genes. Pathway analysis revealed enrichment in genes in duct cells compared to BCs that were related to epithelial development, such as skin and hair development and dermatological conditions and diseases.

C. Validation of the microarray gene expression of candidate genes was performed with quantitative real-time PCR. *K14*, *K5*, *Igfbp4* and *Asprv1* were more highly expressed in duct as compared to basal cells. Data was analyzed using a two-tailed unequal variance Student's t-test. Asterisk indicates a p-value < 0.005. *Dsg11* trended to significance with a p-value of 0.06.

D. Immunofluorescent staining of IGFBP4 and ASPRV1 in tracheal samples confirmed the location of these proteins was mostly in the SMG duct. ASPRV1 is also located in a few apical cells of the SE adjacent to the opening of SMG ducts on the SE.

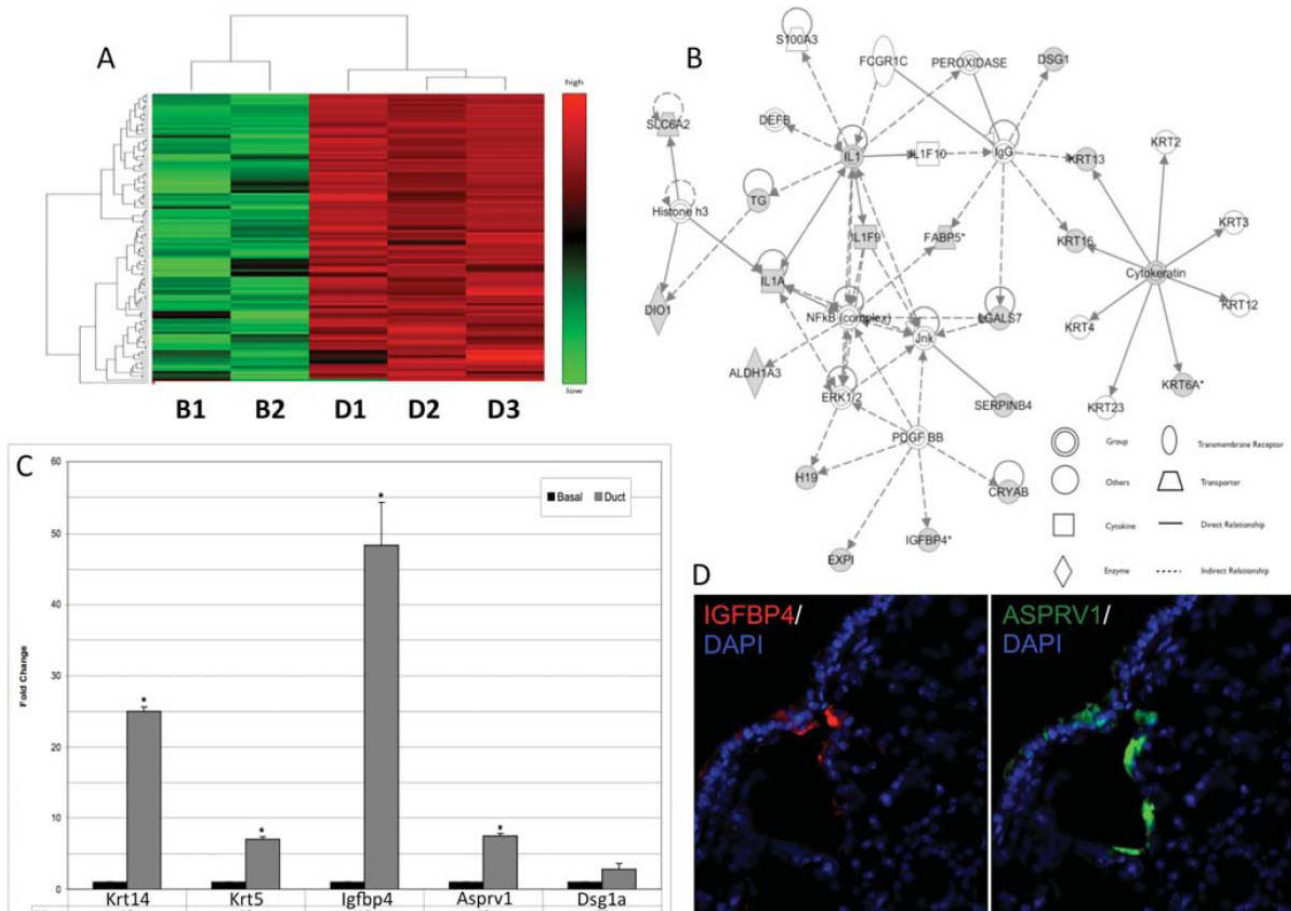


Figure 5. Sorted RFP+TROP-2+ duct cells reconstitute SMG tubule-like and SMG duct-like structures in an *in vivo* regeneration model.

To examine the ability of SMG duct cells to reconstitute SMG-like and SMG duct-like structures *in vivo*, we placed FACS-sorted RFP+TROP-2+ duct cells into the fat pad under the skin of the mouse back. (n=20. 5000 cells per mice). We found that in 50% of the grafts, SMG duct cells could organize themselves into SMG tubule-like structures (i-v) and were RFP+ i.e. of donor origin (i). These SMG-like structures were K5+ and K14+ (ii, v) and expressed the serous cell marker, lysozyme (vi). In 20% of grafts SMG duct-like structures were seen in addition to the typical tubule-like structures (arrows)(ii). Cells around the SMG tubule-like structures expressed K5 and α -SMA, which are markers of myoepithelial cells (v, vi).

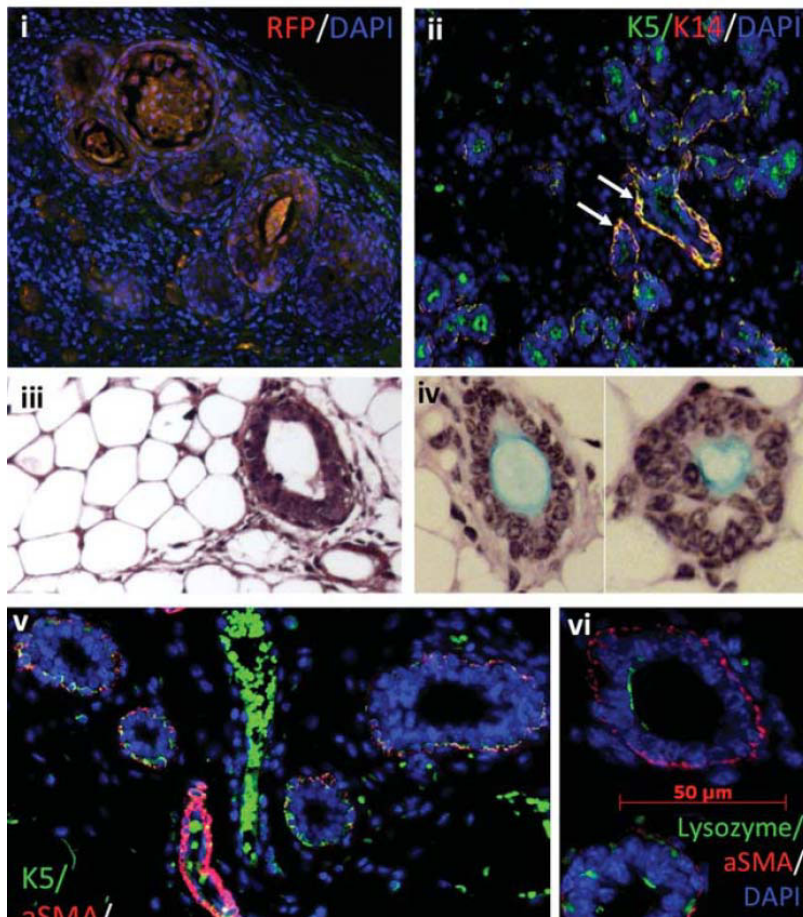


Figure 5

Figure 6. Lineage tracing of K14-YFP expressing cells in the *in vivo* tracheal transplant airway regeneration model after hypoxic-ischemic injury.

In naïve mouse tracheas, cells that express K14 are almost entirely located in the SMG ducts (white arrow) and MECs, and only 10% of SE BCs express K14 (green arrow)(i). To trace the contribution of K14+ SMG duct cells to the repair of the airway epithelium after hypoxic-ischemic injury, we utilized a transgenic mouse model to selectively induce YFP expression in K14-expressing cells. K14CrePR mice [25] were bred with ROSA26-floxed STOP-YFP mice. RU486 or vehicle control was administered intratracheally on day 0. On day 6, tracheas were harvested from these transgenic mice and tracheas were immersed in RU486 or vehicle control, before being transplanted heterotopically into wild-type recipient mice. These tracheal transplants were harvested 7 days later and immunostaining was performed for YFP and K5 and K14 expression. YFP expression was found to co-localize with regions of K14 expression of the SMG, SMG duct and the SE adjacent to and overlying the SMG ducts (ii, iii). In the lower two-thirds of the trachea, which does not have SMGs, a few randomly scattered foci of YFP+K14+ cells were seen in the SE (iv, arrow).

